A novel fuzzy logic variable geometry turbocharger and exhaust gas recirculation control scheme for optimizing the performance and emissions of a diesel engine

Article (Accepted Version)

A novel fuzzy logic VGT and EGR control scheme for optimizing the performance and emissions of a diesel engine

Journal:	*International Journal of Engine Research*
Manuscript ID	IJER-17-0261.R2
Manuscript Type:	Standard Article
Date Submitted by the Author:	27-Sep-2018
Complete List of Authors:	Cheng, Li; University of Sussex Dimitriou, Pavlos; National Institute of Advanced Industrial Science and Technology (AIST), Renewable Energy Research Center Wang, William; University of Sussex Peng, Jun; University of Bedfordshire Aitouche, Abdel; Hautes Etudes d'Ingenieur
Keywords:	EGR, exhaust gas recirculation, VGT, variable geometry, fuzzy logic control, diesel engine
Abstract:	Variable geometry turbochargers (VGT) and exhaust gas recirculation (EGR) valves are widely installed on diesel engines to allow optimized control of intake air mass flow and exhaust gas recirculation ratio. The positions of VGT vanes and EGR valve are predominantly regulated by dual-loop Proportional Integral Derivatives (PID) to achieve predefined set points of intake air pressure and EGR mass flow. The set points are determined by extensive mapping of the intake air pressure and EGR mass flow against various engine speeds and loads concerning engine performance and emissions. However, due to the inherent nonlinearities of diesel engines and the strong interferences between VGT and EGR, an extensive map of gains for P, I, and D terms of the PID controller is required to achieve desired control performance. The present study proposes a novel fuzzy logic control scheme to determine appropriate positions of VGT vanes and EGR valve in real-time. Once determined, the actual positions of the vanes and valve is regulated by two local PID controllers. The fuzzy logic control rules are derived based on an understanding of the interactions among the VGT, EGR and diesel engine. Simulation results obtained from a validated 1D transient diesel engine model showed that the proposed fuzzy logic control scheme is capable of

	efficiently optimizing VGT and EGR positions under transient engine operating conditions in real-time. Compared to the baseline PID controller approach, both engine`s efficiency and total turbo efficiency have been improved by the proposed fuzzy logic control scheme while NOx and soot emissions have been significantly reduced by 34% and 82% respectively.
Note: The following files were submitted by the author for peer review, but cannot be converted to PDF. You must view these files (e.g. movies) online.	
Figs.zip	

A novel fuzzy logic VGT and EGR control scheme for optimizing the performance and emissions of a diesel engine

Li Cheng[1,*], Pavlos Dimitriou[2], William Wang[1], Jun Peng[3], Abdel Aitouche[4]

1. University of Sussex, Department of Engineering & Informatics, Brighton BN1 9QT, UK
2. National Institute of Advanced Industrial Science and Technology (AIST), Renewable Energy Research Center, 2-2-9 Machiikedai, Koriyama, Fukushima 963-0298, Japan
3. University of Bedfordshire, Faculty of Creative Arts, Technologies and Science, Luton, Bedfordshire, LU1 3JU, UK
4. Hautes Etudes d'Ingenieur, Centre de Recherche en Informatique, Signal et Automatique de Lille (CRIStAL), 59046 Lille, France

EGR; exhaust gas recirculation; VGT; variable geometry; fuzzy logic control; diesel engine

Abstract

Variable geometry turbochargers (VGT) and exhaust gas recirculation (EGR) valves are widely installed on diesel engines to allow optimized control of intake air mass flow and exhaust gas recirculation ratio. The positions of VGT vanes and EGR valve are predominantly regulated by dual-loop Proportional Integral Derivatives (PID) controllers to achieve predefined set points of intake air pressure and EGR mass flow. The set points are determined by extensive mapping of the intake air pressure and EGR mass flow against various engine speeds and loads concerning engine performance and emissions. However, due to the inherent nonlinearities of diesel engines and the strong interferences between VGT and EGR, an extensive map of gains for the P, I, and D terms of the PID controllers is required to achieve desired control performance. The present simulation study proposes a novel fuzzy logic control scheme to determine appropriate positions of VGT vanes and EGR valve in real-time. Once determined, the actual positions of the vanes and valve are regulated by two local PID controllers. The fuzzy logic control rules are derived based on an understanding of the interactions among the VGT, EGR and diesel engine. The results obtained from an experimentaly validated 1D transient diesel engine model showed that the proposed fuzzy logic control scheme is capable of efficiently optimizing VGT and EGR positions under transient engine operating conditions in real-time. Compared to the baseline PID controllers approach, both engine`s efficiency and total turbo efficiency have been improved by the proposed fuzzy logic control scheme while NOx and soot emissions have been significantly reduced by 34% and 82% respectively.

1. Introduction

Diesel engines are high-efficiency compression-ignition engines that consume less fuel and produce lower carbon and hydrocarbon emissions compared to spark-ignited petrol engines (1). However, due to the compression-ignition operation, high compression ratios are required for the ignition of fuel which results in increased combustion temperatures and hence high nitric oxides formation (NOx) (2). Several combustion strategies can be found in the literature for the reduction of NOx formation in compression engines such as multiple

injection strategies (3,4), in-cylinder water injection (5), exhaust gas recirculation (6) and others.

Exhaust gas recirculation (EGR) is one of the most effective ways for reducing NOx levels efficiently with relatively low cost. By reintroducing a certain amount of exhaust gas into the inlet manifold, the oxygen concentration is reduced and thus NOx formation is restricted due to a less intense combustion with lower temperature (7). The amount of exhaust gas flowing back to the inlet manifold is controlled by a movable piston valve. An accurate control of the EGR flow is necessary to avoid an oversupply of EGR which can result in a negative effect on soot emission, engine performance, and stability.

For increasing the volumetric efficiency and specific power, modern diesel engines are equipped with an exhaust gas driven turbocharger. The turbocharger is mandatory to perform sufficiently even at the highest operating speeds and loads of the engine (8). This often requires the selection of a big turbocharger with a poor performance at low speed and load conditions which leads to turbo lag effect during transient operation.

A variable geometry turbocharger (VGT) can be used for improving the performance of the engine at low engine speed and load conditions. The movable vanes of the turbine can restrict the gas flow though the turbine and work in a similar manner as a smaller turbine would do. Moreover, this can eliminate the need for a waste-gate as the adjustment of the vanes position can control the pre-turbine pressure of the engine and assist the EGR supply (9).

The adjustment of the movable vanes of the turbine and the EGR valve`s piston is achieved by controllers. The most widely used VGT and EGR controllers in mass-produced ground transport engines are the proportional integral derivative (PID) controllers (10). This control system is often based on a dual-loop PID control structure. The control scheme regulates inlet pressure and EGR ratio based on a number of set points obtained from two predefined maps. One loop uses a feedback signal from an inlet air pressure sensor to control the VGT position while the other uses feedback signals from two flow meters to control the EGR position. However, these two loops cannot work simultaneously due to the highly coupled nature of inlet pressure and flow. In other words, only one loop of the control can be activated depending on the operating condition of the engine. Another drawback of this control method is the fact that a map of PID gains has to be generated in order to cope with the inherent nonlinearity of the diesel engine system and the strong interference between VGT and EGR. This further increases the development and hardware cost of the engine.

Model-based controllers as described in (11), such as predictive controllers (12), multivariable approach (13), and robust controllers (14,15), are able to cope with the nonlinearity of a system well. However, they are relatively more difficult to be applied on a large production scale due to the high variability of engine parameters. Apart from this, mathematical models such as state-space models have to be simplified in order to reduce the computing time. Jankovic et al. (16) built a mean value diesel engine model based on the conservation of mass and energy and the ideal gas law. The authors neglected the heat transfer to the surroundings and several nonlinear functions in the controller were held constant for simplifying its implementation. Abidi et al. (17) developed a state-space diesel engine model for the control of VGT and EGR. For simplifying its performance and reducing the computing cost, the inlet temperature effect was neglected in the model. However, such simplifications sacrifice the accuracy of the models. Meanwhile, control algorithms based on the simplified state-space model are impractical due to the fact that some of the variables required by the model cannot be directly measured, i.e. turbo efficiency (18). As a result, the implementation of these models is only practical for simulation studies or on particular engine operating conditions. Kuzmych et al. (19) developed a robust nonlinear controller based on a control-Lyapunov function. The obtained controller gain guarantees the global convergence of the system and regulates the intake flow and EGR flow in order to minimize

emissions. The simulation results confirmed the effectiveness of this approach. However, due to the nature of this control approach, it is also difficult to be implemented on a real engine.
In the literature, intelligent systems have been proposed to improve the control performance of internal combustion engines. Bai et al. (20) developed an air mass model using a Takagi-Sugeno fuzzy neural network in their coordinated EGR-VGT control system which can predict the charged fresh air mass entering the cylinder. The simulation results of a TDI engine model verifies that the model enables a better control of the intake air mass, and thus improves the air-fuel-ratio control and reduces NOx emission in transients. Apart from this, a fuzzy logic controller proposed by Arnold et al. (10) is capable of controlling the VGT vanes and EGR valve simultaneously without using a model of the air path system, which results in a reduced usage of ECU`s memory by eliminating the need of maps. Simani et al. (21) proposed a fuzzy modeling approach oriented to the design of a fuzzy controller for regulating the fresh airflow of a diesel engine. In comparison to the current PID embedded strategy developed by BOSCH, a significant improvement in desired set-points tracking was obtained. Mastrovito et al. (22) used a multi-agent system (MAS) approach to manage the boost control process of a modern turbocharged diesel engine. The MAS controller performed better than the traditional PID controller in terms of promptness but also showed a good level of adaptivity, precision, robustness and stability. The authors highlighted that the use of fuzzy logic makes it possible to blend computed rules with heuristic rules. Moreover, fuzzy logic controllers have been previously used in diesel engines for controlling several other parameters, such as the urea dosage in a selective catalyst reaction system (23) or predict the engine performance, emission and combustion characteristic of a biodiesel run engine (24).
The controllers described above aim to achieve the optimal intake pressure and flow set-points by regulating the positions of the VGT vanes and EGR valve. Consequently, these controllers require relevant engine calibration to determine the optimal intake pressure and flow at different engine speeds and loads with respect to engine performance and emissions. The proposed fuzzy logic control scheme provides an alternative approach to address the VGT and EGR control problem on a diesel engine. Instead of relying on predefined set-points for the intake air pressure and flow, the control scheme optimizes the VGT and EGR positions based on a set of fuzzy logic control rules developed after comprehensive studies of the interactions among the VGT, EGR and the engine. Two local PID controllers then regulate the VGT and EGR positions based on the control output of the fuzzy logic controller. The proposed approach, rather than indirectly controlling emissions by optimizing the intake pressure and EGR ratio, is directly monitoring the emissions formation and working towards meeting the targeted values. This eliminates complex control software developments and operates in a human decision-making approach.

2. Experimental apparatus

2.1 Test-bed description

A Caterpillar (CAT) 3126B truck engine coupled to a SCHORCH dynamometer was used for the validation of the 1D model used in this study (Table 1). The engine is equipped with a Garrett GT3782VA variable geometry turbocharger and a Pierburg EGR valve. An intercooler and an EGR cooler have been installed on the test bed for cooling the intake air and EGR gas respectively. The main specifications of the engine are listed in Table 1. The engine is connected to two control platforms which are the CP Cadet and the dSPACE control desk. The engine tests are governed by the CP Cadet, which allows operation against a predefined driving cycle and also logs the test conditions and obtained results. The

dSPACE control desk communicates with a MicroAutoBox (model 1401/1501) for data storage and control signals provisioning during the operation of the engine.

Table 1. Specifications of the CAT3126B engine.

Engine model	CAT3126B
Total displacement	7.25L
Type of engine	Inline-4 stroke
Cylinder number	6
Bore * stroke	110*127mm
Compression ratio	16:1
Maximum torque	1166Nm@1440rpm
Maximum power	224kw@2200rpm
Idle/max speed	2640rpm

Apart from the existing sensors built in for ECU and dynamometer control, additional sensors have been installed around the engine and have been wired to the dSPACE MicroAutoBox. These are,

- Two flow meters for measuring the intake air and EGR gas flows
- Two pressure sensors for measuring the inlet and exhaust manifold pressures
- An acceleration pedal position sensor for controlling the engine load
- A shaft encoder for measuring the engine speed
- Two emission analyzers for measuring the soot and NOx levels in the exhaust gas

The accuracy of the emissions analyzers is shown in Table 2. Additionally, the installed VGT and EGR valve are equipped with position feedback sensors.

Table 2. Equipment used for emission measurement.

Sensors	**Accuracy**
AVL 439 opacimeter	Zero-level stability within 0.2%
Testo 350 emission analyzer	±5% of reading (NO, NO2)

Although the accuracy of the NOx emission analyzer is relatively poor, this is not a major issue for this study as the ultimate goal of the 1D model is to predict the trend of the results for evaluating the performance of the fuzzy logic controller.

2.2 Considered diesel engine air-path

The exhaust gas recirculation system of this engine setup is a high-pressure system where the EGR valve is located upstream the turbine while the EGR flow is delivered downstream the compressor. In a high-pressure EGR system, the EGR valve opening results in a reduction of the gas flow passing through the turbine while the maximum amount of EGR rate is dependent on the positive pressure gradient between the exhaust and inlet sides (7). An alternative to the traditional high-pressure EGR system is the low-pressure system. In a low-pressure EGR system, the EGR valve is located downstream the turbine and the flow is delivered upstream the compressor inlet (25). Alternative approaches with the hybrid implementation of the two systems or the implementation of a mid-route EGR system for two-stage boosted engines have also been reported in the literature (26–28). The major air-path components of the Caterpillar 3126B engine test-bed are presented in Figure 1.

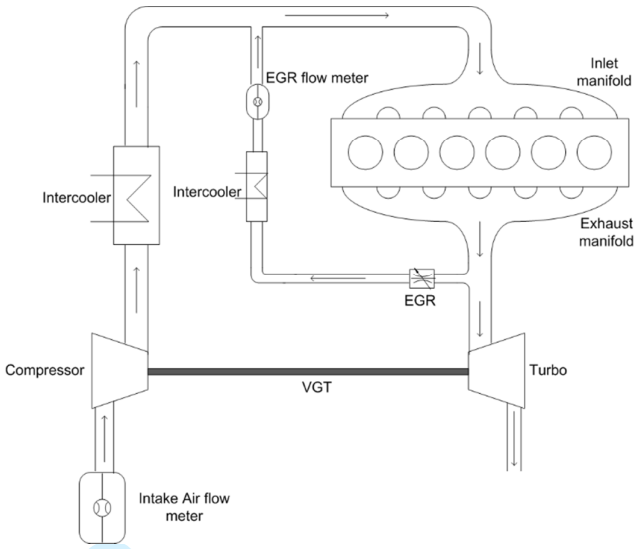

Figure 1. Diesel engine air path.

3. Model description and validation

3.1 1D transient engine model

In this work, a 1D transient engine model (see Figure 2) of the Caterpillar 3126B test-bed has been developed in AVL-BOOST platform. The model was developed based on the considered air path components of the engine as shown in Figure 1. The components of the engine model are fully described in Table 3.

Table 3. Components and their description of the 1D model.

Component	**Description**	**Component**	**Description**
E1	Engine block	PL1 – PL4	Four plenums
C1 – C6	Six cylinders	SB1 – SB3	Three system boundaries
TC1	VGT	J1 – J5	Five junctions
TH1	EGR valve	MP1 – MP14	14 measuring points
CO1 – CO2	Two intercoolers	ECU1	ECU
MHC1	Mechanical consumer	MNT1	Monitor
1 - 30	Pipelines	API1	MATLAB interface

All the components including the diameter and length of the pipes were configured according to the actual test-bed. The model was validated against the experimental results for various engine loads and speeds (see Section 3.3).

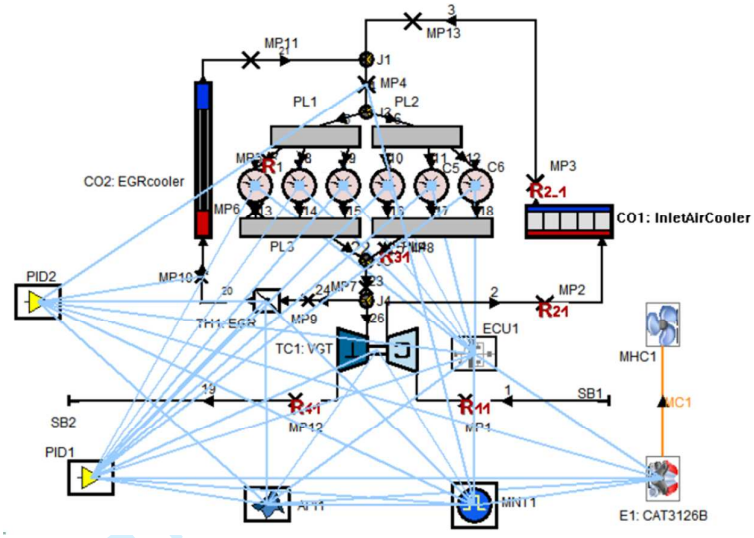

Figure 2. 1D engine model developed in AVL-BOOST.

3.2 Main sub-models' configuration

The configuration of the Engine (E1) and Cylinders (C1 to C6) sub-models are described briefly in Table 4 and Table 5. The engine friction was calculated using the SLM model proposed by Shayler et al. (29). The combustion model used for this simulation is the Vibe 2-Zone. This model calculates two mass average temperatures (burned and unburned zone) and provides a more accurate prediction of the pollutants (NOx, CO, soot). The heat release characteristics are defined by the start of combustion (SOC), combustion duration (CD), shape parameter *m*, and parameter *a*. The values of these parameters were defined against the engine speed at full load and the details are shown in Table 6. The prediction of NOx and soot emissions has been calibrated using the four parameters provided by the emission models which are the NOx kinetic multiplier, the NOx post-processing multiplier, soot the production constant, and the soot consumption constant.

Table 4. Configuration of the Engine sub-model.

General	**Cycle type**	4-stroke
Cylinder setup	**Firing order** **C1-C2-C3-C4-C5-C6**	0 – 480 – 240 – 600 – 120 – 360deg
Engine friction	**Friction model**	Shayler, Leong. Murphy model
	Cylinder arrangement	Inline
	Type of valve train	SOHC-rocker arm
	Number of camshafts bearings	6 camshaft bearings
	Maximum valve lift	12mm
	Type of cam follower	Roller follower
	Oil type	SAE 15W-40 oil at 80degC
	Injection pump	Included

Table 5. Configuration of the Cylinders sub-model.

General	**Bore**	110mm
	Stroke	127mm
	Compression ratio	16
	Con-Rod length	200mm

	Scavenge model	Perfect mixing
Initialization	**Initial pressure at exhaust valve open**	8.5bar
	Initial temperature at exhaust valve open	1248.24K
	Ratio type	Air/fuel ratio
	Ratio value	14.7
	Combustion products	0.628
Combustion	**Heat release model**	Viber 2-zone
	Parameter *a*	6.9
	NOx kinetic multiplier	0.11
	NOx post-processing multiplier	0.3
	Soot production constant	200
	Soot consumption constant	900
Heat transfer	**Cylinder model**	Woschni 1990
	Ports	Zapf
	Combustion system	Direct injection
	In-cylinder swirl ratio nD/nM	1.9

Table 6. Vibe 2-Zone combustion model configuration.

Engine speed, rpm	**700 (Idling)**	**1100**	**2200 (Rated)**	**2640 (Maximum)**
SOC@full load, CRA degree	711.9	710.8	706.8	705.7
CD@full load, CRA degree	55	60	75	81
Shape parameter@full load, *m* (-)	1.04	1	0.9	0.86

The heat transfer at the intake and exhaust ports was calculated using a modified Zapf heat transfer model (30) (see Equation (1) to Equation (3)). The heat transfer coefficient depends on the direction of the air flow. For air flowing out of and into the cylinder, Equation (2) and Equation (3) are adopted respectively.

$$T_d = (T_u - T_w) \cdot e^{\left(-A_w \cdot \frac{\alpha_p}{\dot{m} \cdot c_p}\right)} + T_w \quad \text{Equation (1)}$$

$$\alpha_p = [C_4 + C_5 \cdot T_u - C_6 \cdot T_u^2] \cdot T_u^{0.44} \cdot \dot{m}^{0.5} \cdot d_{vi}^{-1.5} \cdot [1 - 0.797 \cdot \frac{h_v}{d_{vi}}] \quad \text{Equation (2)}$$

$$\alpha_p = [C_7 + C_8 \cdot T_u - C_9 \cdot T_u^2] \cdot T_u^{0.33} \cdot \dot{m}^{0.68} \cdot d_{vi}^{-1.68} \cdot [1 - 0.765 \cdot \frac{h_v}{d_{vi}}] \quad \text{Equation (3)}$$

The selection of the constant values used is shown in Table 7.

Table 7. Constant values used in the modified Zapf heat transfer model.

C_4	1.2809	C_7	1.5132
C_5	7.0451e-004	C_8	7.1625e-004
C_6	4.8035e-007	C_9	5.3719e-007

The configuration of the intake and exhaust ports sub-model is listed in Table 8. The mass flow rates at the intake and exhaust ports were calculated from the equations for isentropic orifice flow considering the flow efficiencies of the ports determined by the steady state flow test rig. Equation (4) to Equation (7) were used to calculate the mass flow rate. For subsonic flow; Equation (5) is substituted into Equation (4); for sonic flow; Equation (6) is substituted into Equation (4).

$$\frac{dm}{dt} = A_{eff} \cdot p_{o1} \cdot \sqrt{\frac{2}{R_0 \cdot T_{01}}} \cdot \Psi \quad \text{Equation (4)}$$

$$\Psi = \sqrt{\frac{k}{k-1} \cdot \left[\left(\frac{p_2}{p_{01}}\right)^{\frac{2}{k}} - \left(\frac{p_2}{p_{01}}\right)^{\frac{k+1}{k}} \right]} \quad \text{Equation (5)}$$

$$\Psi = \Psi_{max} = \left(\frac{2}{k+1}\right)^{\frac{1}{k-1}} \cdot \sqrt{\frac{k}{k+1}} \quad \text{Equation (6)}$$

$$A_{eff} = \mu\sigma \cdot \frac{d_{vi}^2 \cdot \pi}{4} \quad \text{Equation (7)}$$

The flow coefficient varies with the valve lift. The valves lift and timing were calculated from the cam-lobe profiles provided by the manufacturer.

Table 8. Valve ports sub-models' configuration.

	Intake port	**Exhaust port**
Surface area	2513.27mm^2	1452.2 mm^2
Wall temperature	246.85 ºC	246.85 ºC
Inner valve seat diameter	37mm	40mm
Valve clearance	0.38mm	0.64mm
Scaling factor for effective flow area	1.1	0.55
Valve opening	310deg	82deg
Cam length	298deg	336deg
Valve opening shift	7deg	10deg
Valve closing shift	7deg	10deg

The ECU sub-model fuel map is defined based on the CAT3126B engine. The map is a two-dimensional look-up table with two inputs (engine speed and load) and one output (injected fuel amount per cycle) which gives the amount of fuel injected per cycle at a given engine speed and load. However, it is essential for the overall air/fuel ratio governed by the ECU sub-model to be maintained above 12 at all times. To build this map, the air intake behavior of the engine without the turbocharger and EGR valve was firstly studied, and the air intake mass flow curves were derived. The fuel map was then developed based on the air intake curves and further adjusted based on the experimental data.
The VGT sub-model was configured using the 'full model' method. The full model option predicts the performance and efficiency of the turbocharger based on the compressor and turbine maps derived from an engine gas stand.

3.3 Model validation

The engine model was validated against experimental results of the Caterpillar 3126B engine at various operating conditions. For this work, a perfect match between simulation and experimental results is not necessary as the engine model is used for understanding the performance and emissions trend. The model is only used as a platform for developing and evaluating the controllers and not improving the engine itself. However, the validation process is necessary to confirm that the model is robust and reliable, and it behaves and performs in a similar manner to the real engine.
In order to acquire the data that can be used to validate the engine model, two sets of experimental tests were carried out on the test-bed. The load demand, VGT, and EGR settings are listed in Table 9. During each set of the engine tests, the engine speed was fixed as 1000 rpm, 1250 rpm, 1440 rpm, 2000 rpm, and 2400rpm respectively. At each engine speed, the steady-state readings of inlet pressure, engine torque, soot, and NOx were

recorded. These are the parameters used to validate the engine model. The simulation results were compared with the experimental data to validate the engine model.
In each set of simulations, the load and EGR position of the engine model were set according to the values listed in Table 9. At each engine speed, VGT position was controlled by a PID controller to achieve the same inlet pressure as it was measured on the engine test-bed.

Table 9. Experiments carried out on the Caterpillar 3126B engine test-bed to collect the data required for the model validation, '100' means fully open, '0' means fully closed (100% load equals to a load demand of 1 as shown in Figures 10 and 11).

	Load, %	VGT position, %	EGR position, %
Set 1	100	100	0
Set 2	100	100	100
Set 3	100	40	0
Set 4	100	40	100

Once the targeted inlet pressure is achieved and stabilized, the values of the other three parameters were recorded and compared with the experimental results. This validation process mainly aims to understand,

1. Whether the air intake behavior of the engine model is in good agreement with that of the CAT3126B engine. At the same engine speed, if the inlet pressure is the same, according to the ideal gas law, the air mass flow should be the same, given that the inlet temperature is the same;
2. Whether the fuel injection map is set correctly compared to the fuel injection of the engine. This can be found out by comparing the mass of fuel injected per second and AFR between the simulation results and the experimental results;
3. Whether the emission models for soot and NOx have been calibrated correctly compared to the real engine measurements.

Figure 3 to Figure 6 show the compassions of inlet pressure, engine torque, normalized soot (see Appendix), and NOx between the simulation and experimental results at Set 1-4 engine operating conditions for different EGR and VGT positions.

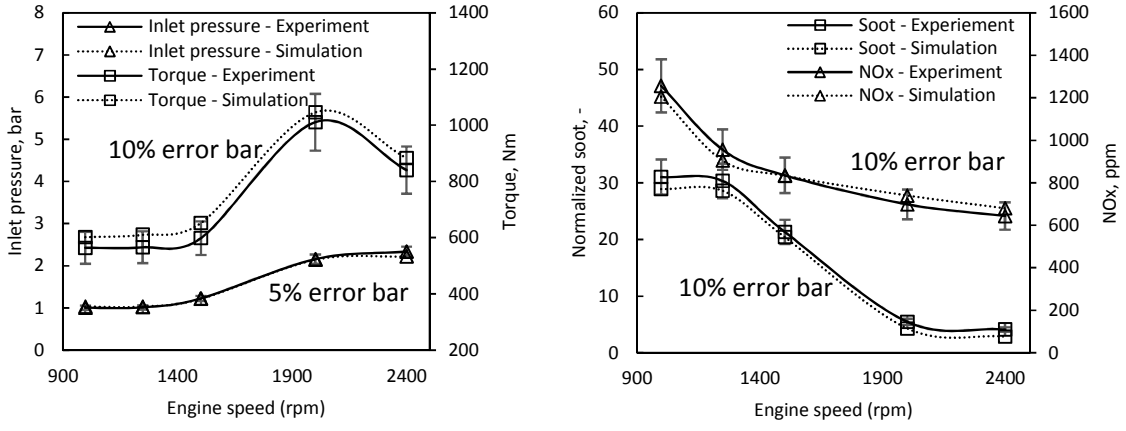

Figure 3. Model validation based on Set 1 engine operating conditions, (a)inlet pressure and torque, (b) soot and NOx emissions.

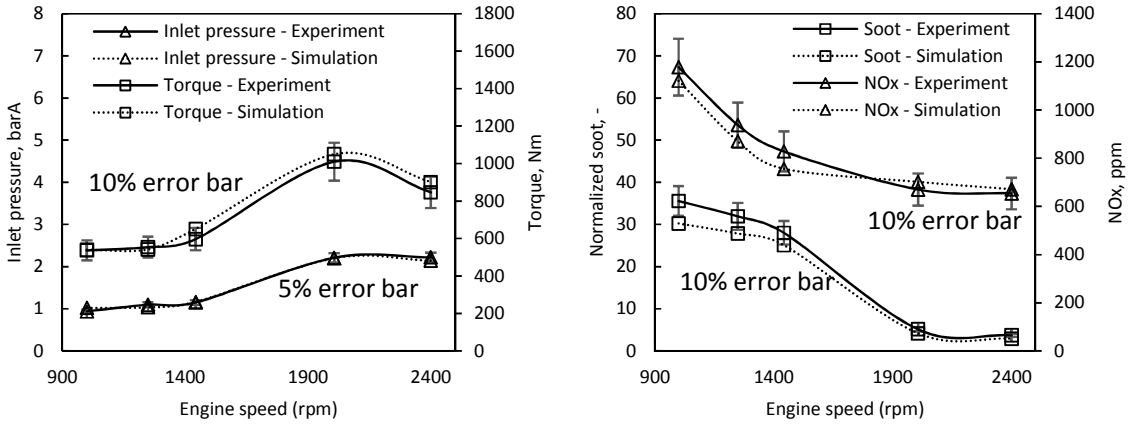

(a) (b)

Figure 4. Model validation based on Set 2 engine operating conditions, (a)inlet pressure and torque, (b) soot and NOx emissions.

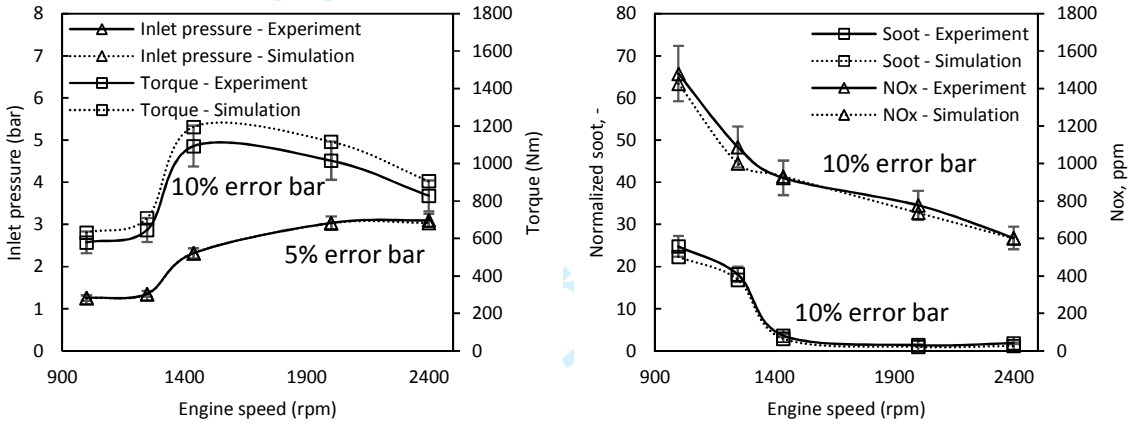

(a) (b)

Figure 5. Model validation based on Set 3 engine operating conditions, (a)inlet pressure and torque, (b) soot and NOx emissions.

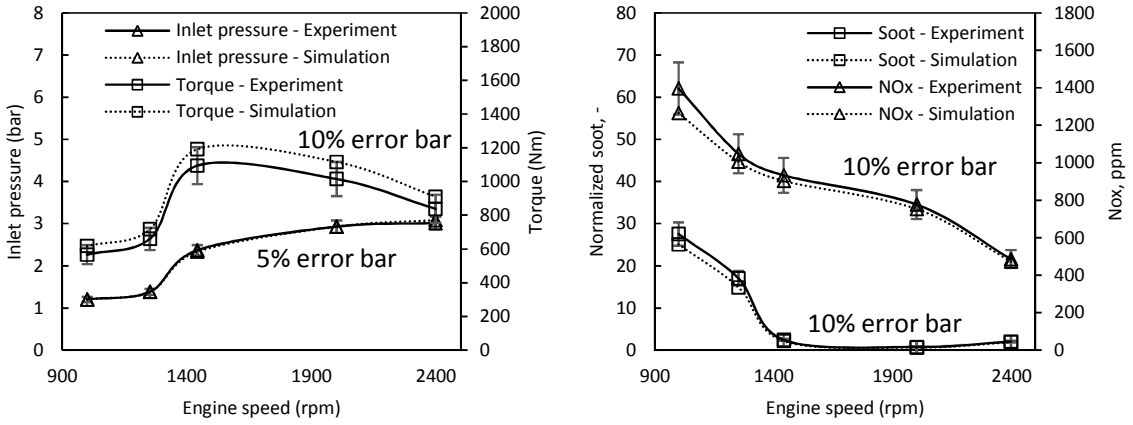

(a) (b)

Figure 6. Model validation based on Set 4 engine operating conditions, (a)inlet pressure and torque, (b) soot and NOx emissions.

Although the error between simulation and experimental results is sometimes relatively high, the trend of the simulated results is in good agreement with the experimental readings for all

the conditions tested. This can confirm a trustworthy model that can be used for assessing the performance of the proposed fuzzy logic controller.

4. Proposed fuzzy logic control scheme

4.1 Overall control structure

A Sugeno-type fuzzy logic control scheme (31) has been developed to control the VGT vanes and EGR valve for improving engine`s fuel consumption and reducing emissions under real-time transient operating conditions. The overall control structure is shown in Figure 7. The fuzzy logic controller receives real-time transient signals from the engine such as speed, load, inlet pressure, soot, and NOx readings which work as the input variables for the controllers. After receiving the input parameters, the controller generates transient vanes and valve position output signals based on a set of predefined fuzzy rules. Two PID controllers are implemented to position the VGT vanes and EGR valves at the position requested by the fuzzy logic controller.

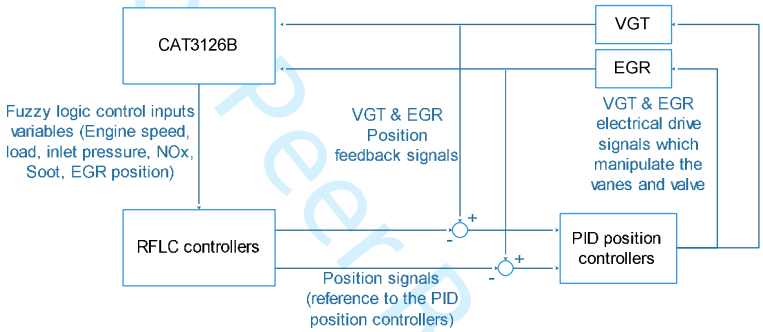

Figure 7. Overall closed-loop fuzzy logic control structure.

4.2 Control rules development

4.2.1 Definition of control variables and membership functions

For the purpose of devopling a fuzzy logic controller, necessary control input and output variables need to be defined. Based on experimental investigations, a total of six control input variables have been defined which are,

1. Engine speed (rpm)
2. Engine load (% demand)
3. Inlet pressure (bar)
4. Opacity (smoke levels)
5. NOx emission (ppm) and
6. EGR position (%)

Two control output variables have been defined which are,

1. VGT vanes position and
2. EGR valve position

A symmetric Gaussian function has been applied for each control input variable which is defined by two parameters, σ and c as given by Equation (8). The output variables membership functions are the Sugeno constant type.

$$f(x;\ \sigma, c) = e^{\frac{-(x-c)^2}{2\sigma^2}} \quad \text{Equation (8)}$$

Table 10 presents the five constant membership functions defined for the VGT position and the three functions for the EGR position variables.

Table 10. Membership functions and their levels for VGT vanes and EGR valve position.

Variable	Membership functions	Vanes/valve position (%)
VGT and EGR	Fully open	100
VGT	Open	75
VGT and EGR	Middle	50
VGT	Closed	25
VGT and EGR	Fully closed	0

4.2.2 Control Rules for VGT and EGR position

The existing VGT PID control approach aims to produce the boosted pressure required without considering the actual working condition of the turbocharger. However, it is essential the following factors to be considered:

1. Restrict the operation of compressor beyond the surge and choke lines to avoid turbocharger failure. This is addressed by Rules 1-3 listed in Figure 8.
2. Restrict excessive boosting to avoid engine failure. This is addressed by Rules 9 and 10 listed in Figure 8.
3. Keep the VGT open whenever possible to reduce unnecessary pumping losses. This is addressed by Rules 4-8 and 11-15 listed in Figure 8.
4. Achieve high enough back pressure to achieve targeted EGR rates. This is addressed by Rules 16-18 listed in Figure 8.

Considering all control requirements listed above, a total of 18 fuzzy logic rules, presented in Figure 8, have been proposed for the VGT control.

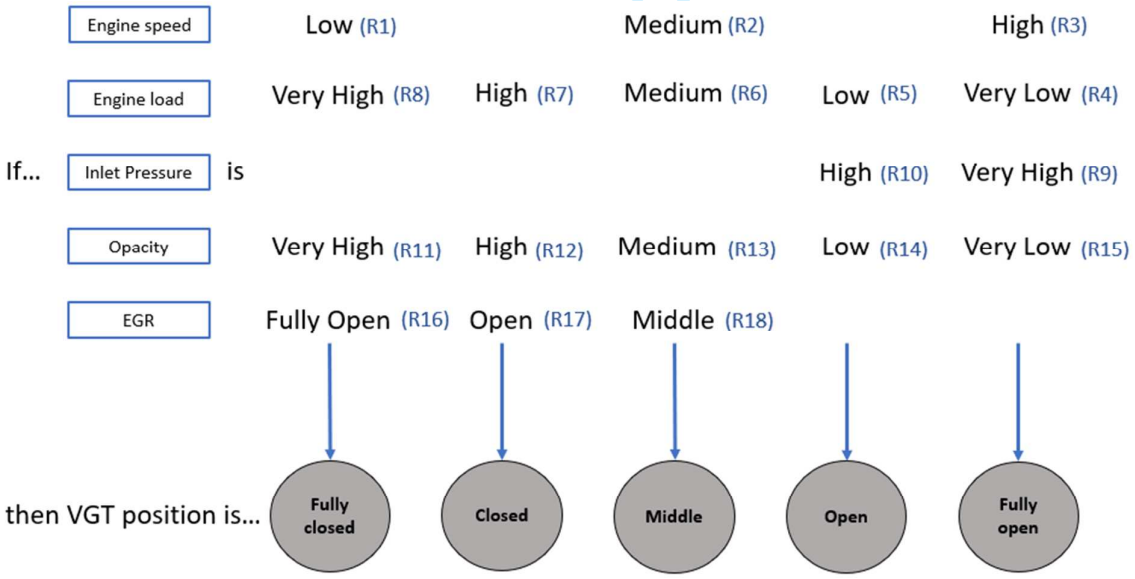

Figure 8. Fuzzy logic control rules for EGR and VGT position (R stands for Rule).

Rules 1-3 govern the VGT position with respect to the engine speed. When selecting a turbocharger, it is mandatory to be of the right size for operating even at extreme engine speed and load conditions. As a result, when the engine is operating in the low-speed range,

the reduced exhaust gas flow does not have sufficient energy to propel the turbine wheel. For this reason, the vanes of the turbine need to be positioned in the closed range to represent a smaller size turbocharger. On the other hand, at high engine speeds, the VGT vanes should be positioned in the open range. This will prevent the compressor from working beyond the choke line which is an indication of deteriorated efficiency. This can also reduce back pressure which leads to reduced pumping losses.

Rules 4-8 govern the VGT position with respect to the engine load. When the engine is running at a high load, the demand for fuel and oxygen is higher. In order to supply the engine with the required oxygen, the VGT vanes should be positioned in the closed range. When the load is low, the demand for fuel and oxygen levels are relatively low. Consequently, the VGT vanes should be positioned towards the open range for reducing pumping losses.

Rules 9 and 10 set the boost pressure limit of the engine. When the boost pressure is approaching the maximum allowed limit, the VGT vanes must move towards the open position for avoiding engine`s failure.

Rules 11-15 adjust the VGT position with respect to the opacity of the exhaust gas. These rules are placed to provide a higher boost pressure, and hence oxygen for soot oxidation, when the opacity of the exhaust gas exceeds the predefined values.

Rules 16-18 adjust the VGT position with respect to the EGR valve position. This allows producing the necessary back pressure needed for recirculating part of the exhaust gas to the inlet manifold through the EGR valve.

High recirculated exhaust gas rates can have a significant adverse effect on the engine performance. Therefore, the control of EGR should adequately address the trade-off between emissions and performance which is to minimize the effect on the performance of the engine while reducing NOx formation. Based on experimental studies, the EGR valve should only be opened during medium engine speeds with high NOx emission conditions. The following three fuzzy logic control rules have been proposed for the EGR control,

1. If ENGINE SPEED is **medium** and LOAD is **medium,** and NOx is **not low**, then EGR POSITION is ***Open***
2. If ENGINE SPEED is **medium** and LOAD is **medium,** and NOx is **low**, then EGR POSITION is ***Closed***
3. If ENGINE SPEED is **not medium** and LOAD is **not medium**, then EGR POSITION is ***Closed***

4.3 Control outputs

The control outputs of the controller are the required positions of the VGT vanes and EGR valve. Each control decision is made by computing the final output of the Sugeno fuzzy inference system. The Sugeno (also known as Takagi-Sugeno) method of fuzzy inference was introduced in 1985 (32), and the output membership functions are either linear or constant. For this controller, because of the constant type of output variables, the fuzzy model is of the form,

If Input 1 = x, Input 2 = y, … , Input n = r, then the output is $z = c$ (c is a constant)

The output level z of each rule is weighted by the firing strength w of the rule, which can be acquired by Equation (9).

$$w_i = AndMethod(F_1(x), F_2(y), \dots, F_n(r)) \quad \text{Equation (9)}$$

where $F_1(x), F_2(y), \dots, F_n(r)$ are the membership functions for inputs 1, 2, … , n.

The final output of the fuzzy inference system is the weighted average of all rule outputs, which is given by Equation (10).

$$Final\ output = \frac{\sum_{i=1}^{N} w_i z_i}{\sum_{i=1}^{N} w_i} \qquad \text{Equation (10)}$$

where N is the number of rules.

4.4 VGT and EGR position local control

The VGT and EGR installed on the test bed have feedback channels which monitor the actual positions of the VGT vanes and EGR valve. Two local PI controllers were built to regulate the positions of the vanes and valve. Figure 9 shows the VGT vanes and EGR valve positions against the set points generated by the fuzzy logic controller. It shows that the VGT and EGR positions have followed the position references generated by the proposed fuzzy logic controller within acceptable errors. It is worth mentioning that using PID controllers to regulate VGT and EGR positions is easier than regulating inlet pressure and mass flow due to that fact that fewer nonlinearities are involved.

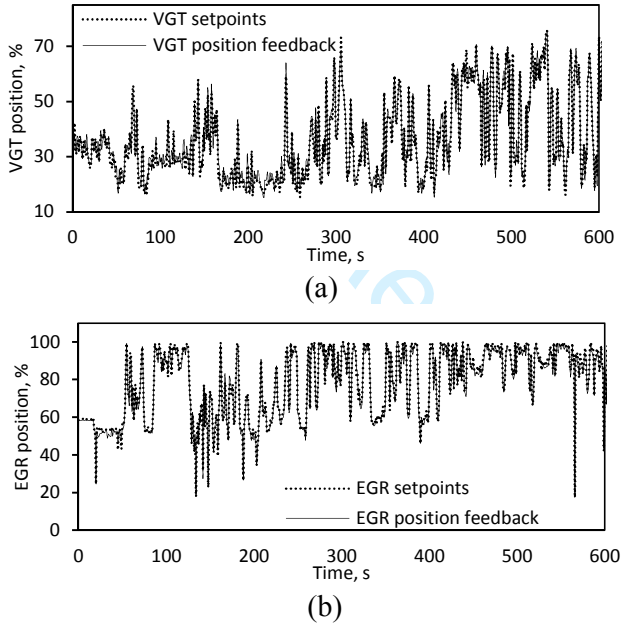

Figure 9. Performances of the local PI controllers: (a) VGT control, (b) EGR control.

5. Results and discussions

5.1 Proposed control scheme compared to PID control

The PID control technique is the most dominating structure of feedback control at present (33). In this study, the PID control technique has been chosen as the baseline to assess the effectiveness of the proposed fuzzy logic control scheme. Map set-points for VGT and EGR mass fraction, Equation (11), control are generated by predefined tables that take engine speed and load demand as input signals. The predefined maps were developed to optimize the

engine`s efficiency and reduce emissions with reference to the trade-off between NOx, soot, and brake specific fuel consumption (BSFC).

$$EGR\ mass\ fraction = \frac{\dot{m}_{EGR}}{\dot{m}_{total\ intake\ air\ flow}} \quad \text{Equation (11)}$$

In order to generate the required set-points of inlet pressure and EGR mass fraction, investigations of how AFR and EGR mass fraction affect the engine performance and emissions have been carried out using the transient engine model. Results show that high AFR lead to increased torque, better fuel consumption, less soot, but higher NOx levels. On the other hand, high EGR mass fractions, lead to low AFR, in-cylinder temperatures, BMEP and higher BSFC with increased soot and reduced NOx emissions. Therefore, a compromise has to be made when determining the appropriate AFR and EGR mass fraction values. The set-points of AFR and EGR mass fraction selected are those producing the lowest possible combination of both soot and NOx emissions. Figure 10 shows the set-point maps generated for the PID control.

As discussed and suggested by both Arnold et al. (10) and Diverak et al. (34), due to the negative impact of the EGR gas on the performance and stability of the engine, EGR valve should only be opened within a restricted area of the set-points map. In this study, the EGR valve opens only when the following conditions are met,

1. Engine speed is between 1400rpm and 2200rpm, and
2. Load demand is less than 0.5.

Similar conditions have been incorporated in the fuzzy logic control rules for the EGR control (see section 4.2.2). However, the definitions of the range of engine speed and load are not as explicit as it has been defined above. Instead, fuzzy set and membership function (35) were used to describe the range of the engine speed and load in fuzzy logic control. In fuzzy logic control, a statement is described by a matter of degrees between 1, and 0 rather than an explicit number.

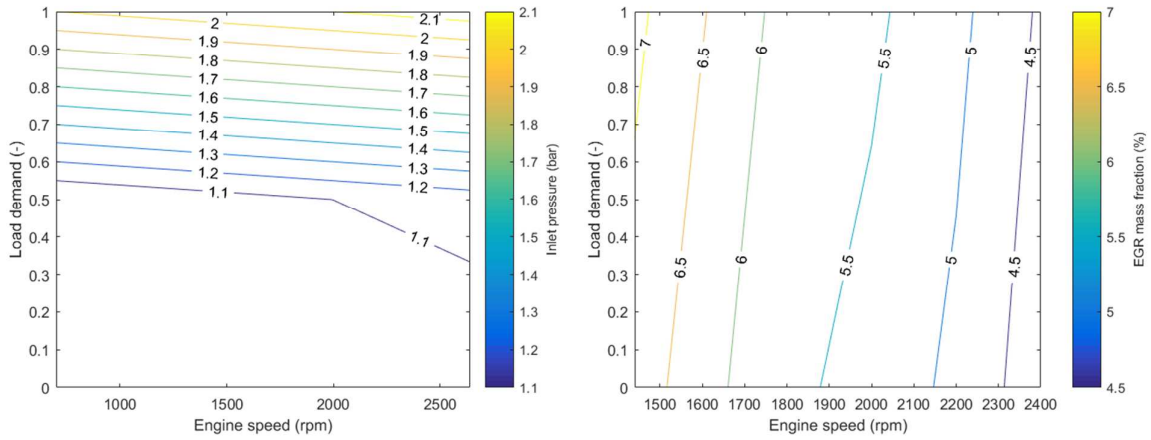

(a) (b)

Figure 10. Set-points maps generated for PID control: (a) inlet pressure map; (b) EGR mass fraction map.

Due to the strong interference between the VGT and EGR valve in a production PID controllers system, the VGT is controlled dependently on the status of the EGR valve (10). In order to assess this interference between the VGT and EGR valve, the following two PID controllers were deployed,

- PID controller 1, VGT vanes position is controlled dependently on the status of the EGR valve;
- PID controller 2, VGT vanes position is controlled independently on the status of the EGR valve.

The responding performances of the PID controller 1 and 2 were assessed under transient simulation mode. In transient simulation mode, a load demand curve needs to be defined. The torque produced by the engine will depend on the load demand curve defined. The change in engine speed is proportional to the difference between the torque produced by the engine and the torque of the resistance load. A positive difference induces an increase in engine speed, whereas a negative difference induces a decrease in engine speed.

In order to evaluate the controllers under different engine operating conditions, the load demand trace used covers various driving patterns such as sharp load change, normal load change, and cruise. Besides, the simulations cover almost the full range of engine speeds and torques. The load demand curve is shown in Figure 11.

The coefficients for P, I, and D terms were tuned at various operational points to achieve the desired control performance considering the rising time, overshoot, settling time, steady-state error and stability (36).

Figure 12 and Figure 13 show the responding performance of these two PID controllers. It can be seen that with the same gain schedules for P, I, and D terms, the control responding performances of the PID controller 1 are better due to fewer interactions between the VGT and EGR control. However, because the VGT vanes have to be kept open when the EGR valve is open (see Figure 14), the engine performance and emissions output are worse than that in the PID controller 2. This was the reason that in this paper, the fuzzy logic controller was compared with PID controller 2.

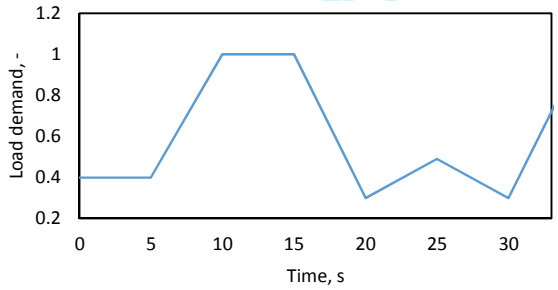

Figure 11. Load demand curve used to compare the fuzzy logic control scheme and the PID controller.

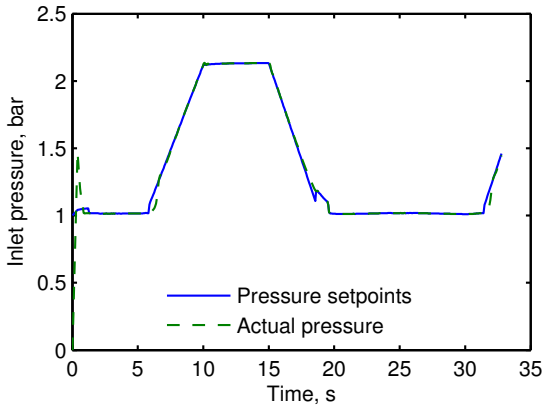

(a)

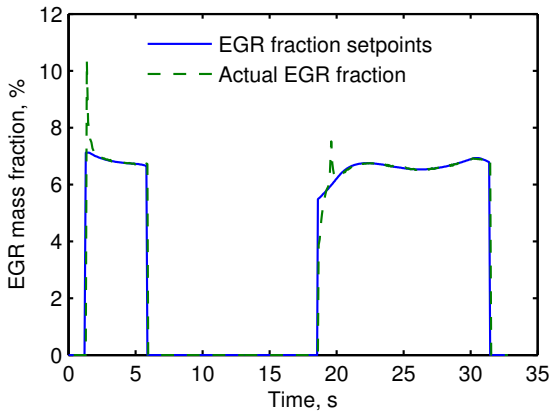

(b)

Figure 12. Responding performances of the PID controller (PID control 1). (a) Actual inlet pressure against set-points; (b) actual EGR mass fraction against set-points.

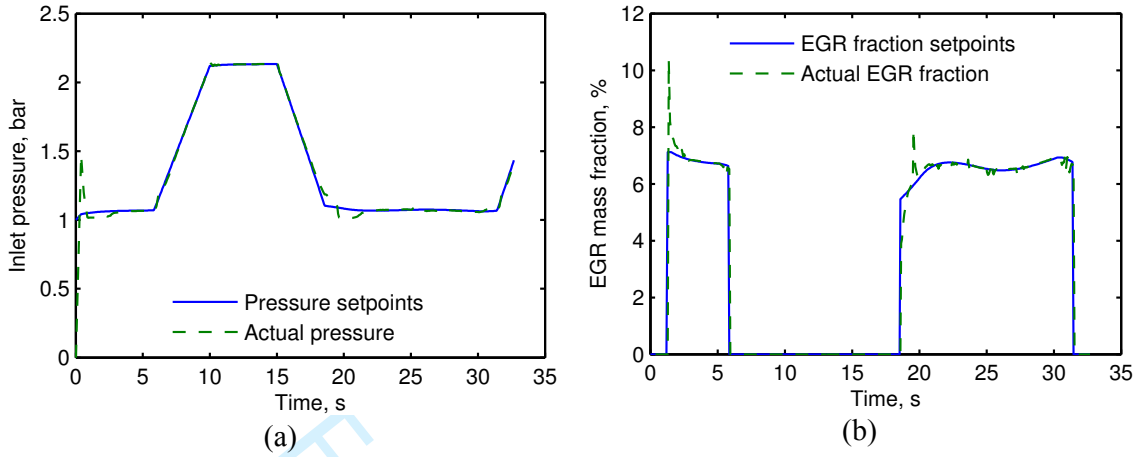

(a) (b)

Figure 13. Responding performances of the PID controller (PID control 2): (a) actual inlet pressure against set-points; (b) actual EGR mass fraction against set-points.

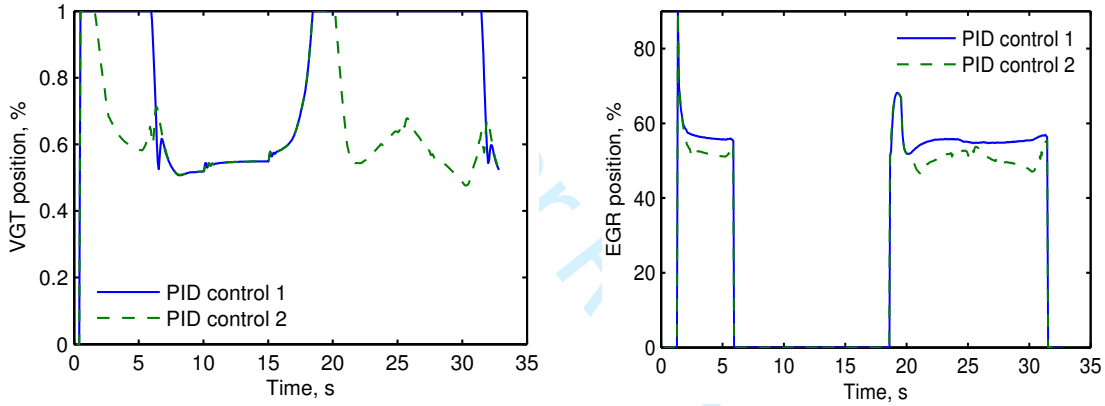

(a) (b)

Figure 14. Comparisons of the VGT position and EGR valve position between PID controller 1 and PID controller 2.

The simulations were set to transient running mode. Figure 15 shows the comparison of simulation results between the fuzzy logic control scheme and the PID control baseline testing under the same load demand curve (Figure 11). The comparison investigates the differences in performance and emissions output of the engine between the control approaches. The fuzzy logic control scheme controls the VGT and EGR based on predefined fuzzy logic rules while the baseline PID controllers' system aims to achieve the predefined optimal inlet pressure and EGR mass fraction by regulating the VGT vanes and EGR valve.

Figure 15(a) presents the comparison of the VGT positions between the fuzzy logic control scheme and the conventional system. The variation range of the VGT position between the two control systems is in the range of 0.2 to 0.6 while at around 10-15, 20 and 30 seconds is of the same level. However, the VGT positions of the fuzzy logic control scheme were generally lower than that of the PID control. This is attributed to the fuzzy logic control Rule 12 and Rule 13 which are defined to reduce the soot emission as much as possible without ignoring turbocharger`s efficacy and safety.

Figure 15(b) shows that the EGR valve position of the model with fuzzy logic control scheme varied more actively compared to that of the PID controller during the whole transient period.

The EGR valve was closed suddenly at around 6s by the PID controller but it was kept open until around 10s by the fuzzy logic controller. This was caused by the explicit definition of the engine speed range of the PID controller as mentioned earlier. Similarly, the EGR valve opened earlier at around 15s by the fuzzy logic controller compared to 18s for the PID controller. The fuzzy set and membership function concepts introduced by the fuzzy logic control have shorten the closing period of the EGR valve, and this has reduced the NOx emissions compared to the conventional system.

Figure 15(c) shows the engine speed and torque traces comparison between the fuzzy logic control scheme and the conventional system for the same load demand (Figure 11). It can be seen that both of the engine speed and torque traces of fuzzy logic control scheme almost overlap the traces of the engine with the conventional system. At around 25s, both of engine speed and torque of the fuzzy logic-controlled engine are slightly higher than that of the baseline PID controller. This is happening although the fuel amount injected for both approaches is the same (Figure 15(d)) which translates to a more useful work performed by the engine when VGT and EGR are controlled by the fuzzy logic scheme.

Figure 15(d) shows the comparisons of the injected fuel mass and AFR of the engine between the fuzzy logic and conventional control systems. The injected fuel mass curves are identical reflecting the same load demand. On the other hand, the AFR of the engine with the fuzzy logic control scheme is higher than the conventional system as a result of applying the fuzzy logic control rules. This increased AFR has significantly contributed on the reduction of the engine`s soot formation.

Figure 15(e) illustrates the engine BSFC and turbo total efficiency traces, Equation (12). It can be seen that the BSFC of the engine with the fuzzy logic scheme is generally lower than that of the engine with the conventional system. This suggests a higher engine efficiency, especially at around 25s of the test. The turbo total efficiency of the fuzzy logic control scheme was maintained at around 0.3 which is higher than that of the conventional system particularly during the first five seconds and between 20s and 30s of the test.

$$\eta_{TC} = \eta_{m,TC} \cdot \eta_{s,T} \cdot \eta_{s,C} \qquad \text{Equation (12)}$$

where η_{TC} is the mechanical efficiency of the turbocharger,
$\eta_{s,T}$ is the isentropic turbine efficiency and
$\eta_{s,C}$ is the isentropic efficiency of the compressor.

Finally, Figure 15(f) shows the soot and NOx emissions produced during the test. It can be seen that both NOx and soot emissions produced by the engine with the fuzzy logic control scheme were lower than that of the conventional system, especially at medium to high engine speed and torque ranges. The reduction of NOx and soot emissions was in the range of 34% and 82% on average during the whole transient period events.

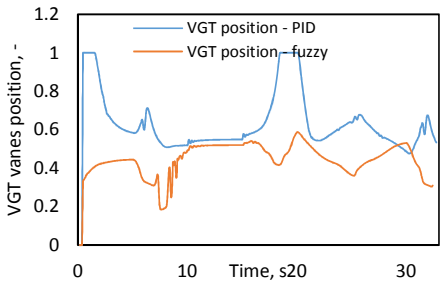

(a)

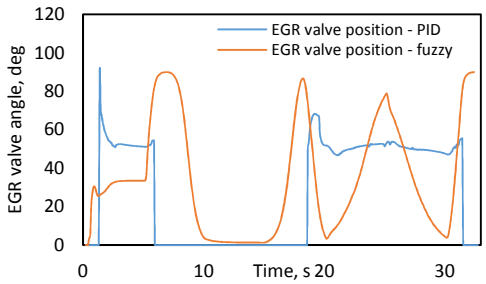

(b)

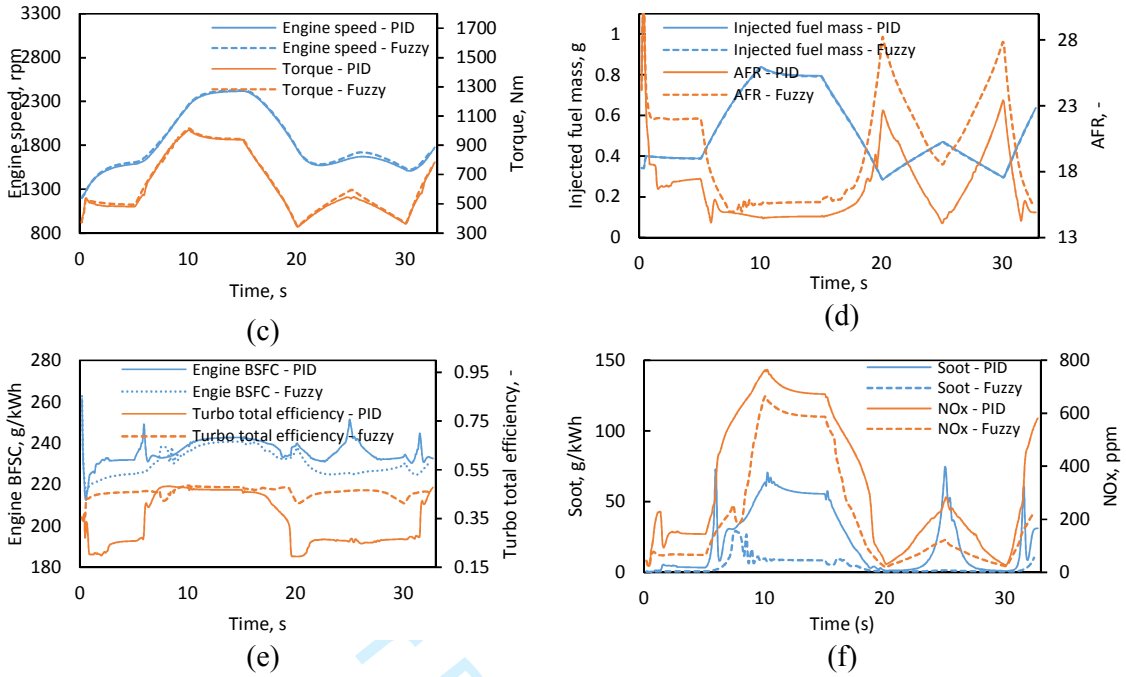

Figure 15. Fuzzy logic control compared to PID control. VGT vanes position: 1 – fully open, 0 – fully closed; EGR valve position: 90deg – fully open, 0deg – fully closed.

6. Conclusions

In this paper, a novel fuzzy logic control scheme has been proposed and tested. The control scheme consists of a fuzzy logic control strategy and two local PID controllers. The fuzzy logic control strategy determines the positions of the VGT vanes and EGR valve in real-time with the aim to optimize the engine`s efficiency and emissions output by considering the trade-off between NOx and soot emissions, and the trade-off between NOx and engine BSFC. The strategy relies on a set of fuzzy logic control rules which were developed based on comprehensive studies of the interactions between the VGT, EGR, and the engine. The actual positions of the VGT vanes and EGR valve are then controlled by two local PID controllers. It takes less effort for the local PID controllers to regulate the VGT and EGR positions against set-points of position than to regulate the VGT and EGR positions against set-points of intake air pressure and EGR rate due to fewer complexities and nonlinearities. The robustness of the fuzzy logic control scheme has been evaluated and published in (37).

The proposed control scheme requires soot and NOx measurements as control input signals. These signals can be made available by using either actual or virtual sensors. Virtual sensors for predicting Soot and NOx concentrations have been well discussed in the literature (38–40), while actual sensors are available for automotive applications.

The effectiveness of the proposed control scheme has been assessed by comparing it with the conventional PID controllers' approach on a 1D transient diesel engine model developed using AVL-BOOST software. The main conclusions obtained from the simulation results are:

1. Under transient simulation mode, the engine speed and torque curves of the fuzzy logic control scheme and the baseline PID control approach almost overlap each other when the same load demand is provided. Although the injected fuel mass was the same, at low to middle engine speed ranges, the engine speed and torque of the baseline PID control were slightly lower than that of the fuzzy logic control scheme.

This can be due to a number of differences on AFR, turbo total efficiency, and EGR valve positions between the two approaches;

2. The total turbo efficiency of the fuzzy logic control scheme was higher than that of the baseline PID control approach. On the other hand, the BSFC of engine with the fuzzy logic control scheme was lower, especially under acceleration events;
3. The soot and NOx emissions of the engine controlled by the fuzzy logic control scheme were both lower by 34% and 82% respectively than that of the baseline PID control approach. This high reduction occurs mainly during the acceleration conditions. However, it is advised as future work that the level of reduction to be confirmed in a higher fidelity 1D model.

Finally, the research work presented in the paper showed that the fuzzy logic controller can improve engine`s efficiency and reduce soot and NOx emissions compared to the PID controllers' approach. On the other hand, this also can suggest that the predefined set-points maps used for the conventional control system could be potentially improved with the aid of the proposed fuzzy logic control rules which consider additional factors such as turbo efficiency, back pressure and others.

7. Acknowledgments

This research work was produced in the framework of SCODECE (Smart COntrol and Diagnosis for Economic and Clean Engine), a European territorial cooperation project part funded by the European Regional Development Fund (ERDF) through the INTERREG IV A 2 Seas Programme. The authors acknowledge the AVL Company to provide computational resources for this research. The financial support of the Daiwa Anglo-Japanese Foundation and the Great Britain Sasakawa Foundation was crucial for the completion of this paper and is highly appreciated.

8. Nomenclature

Symbols

a	characterizing the completeness of the combustion
A_{eff}	effective flow area
A_w	port surface area
C_p	specific heat at constant pressure
d_{vi}	inner valve seat diameter
$\frac{dm}{dt}$	mass flow rate
h_v	valve lift
k	ratio of specific heats
m	shape parameter

$\dot{m}$	mass flow rate
p_{o1}	upstream stagnation pressure
p_2	downstream static pressure
R_0	gas constant
T_{o1}	upstream stagnation temperature
T_d	downstream temperature
T_u	upstream temperature
T_w	port wall temperature
α_p	heat transfer coefficient in the port
$\mu\sigma$	flow coefficient of the port

Acronyms

BDC	bottom dead center
BSFC	brake specific fuel consumption
CAT	Caterpillar
CD	Combustion duration
ECU	electronic control unit
EGR	exhaust gas recirculation
MAS	multi agent system
PID	proportional integral derivative
SFC	specific fuel consumption
SOC	start of combustion
TDC	top dead center
VGT	variable geometry turbocharger

9. References

1. Robert Bosch GmbH. Diesel Engine Management. Book. 2006. 501 p.
2. Heisler H. Advanced Engine Technology. Butterworth-Heinemann Ltd.; 2006.
3. Dimitriou P, Burke R, Copeland CD, Akehurst S. Study on the Effects of EGR Supply

Configuration on Cylinder-to-Cylinder Dispersion and Engine Performance Using 1D-3D Co-Simulation. SAE Tech Pap. 2015-32-0816;2015.
4. Dimitriou P, Peng Z, Wang W, Gao B, Wellers M. Effects of advanced injection strategies on the in-cylinder air-fuel homogeneity of diesel engines. Proc Inst Mech Eng Part D J Automob Eng. 2015;229(3):330-341.
5. Maiboom A, Tauzia X. NOx and PM emissions reduction on an automotive HSDI Diesel engine with water-in-diesel emulsion and EGR: An experimental study. Fuel. 2011;90(11):3179–92.
6. Abd-Alla GH. Using exhaust gas recirculation in internal combustion engines: a review. Energy Convers Manag. 2002;43(8):1027–42.
7. Maiboom A, Tauzia X, Hétet J-F. Experimental study of various effects of exhaust gas recirculation (EGR) on combustion and emissions of an automotive direct injection diesel engine. Energy [Internet]. 2008;33(1):22–34. Available from: http://linkinghub.elsevier.com/retrieve/pii/S0360544207001399
8. Challen B, Baranescu R. Diesel engine reference book. 2nd ed. Elsevier Ltd and A.E. Joyce Ltd.; 1999.
9. Rakopoulos CD, Giakoumis EG. Diesel engine transient operation: Principles of operation and simulation analysis. Diesel Engine Transient Operation: Principles of Operation and Simulation Analysis. 2009. 1-390 p.
10. Arnold JF, Langlois N, Chafouk H. Fuzzy controller of the air system of a diesel engine: Real-time simulation. Eur J Oper Res. 2009;193(1):282–8.
11. Van Nieuwstadt MJ, Kolmanovsky I V., Moraal PE, Stefanopoulou A, Janković M. EGR-VGT control schemes: Experimental comparison for a high-speed diesel engine. IEEE Control Syst Mag [Internet]. 2000;20(3):64–79. Available from: http://www.scopus.com/inward/record.url?eid=2-s2.0-0033728252&partnerID=tZOtx3y1
12. Tschanz F, Amstutz A, Onder CH, Guzzella L. Feedback control of particulate matter and nitrogen oxide emissions in diesel engines. Control Eng Pract. 2013;21(12):1809–20.
13. Gayaka S, Yao B, Meckl PH. A multivariable approach to EGR-VGT actuator control problem. In: ASME International Mechanical Engineering Congress and Exposition. Chicago, Ilinois, USA: ASME; 2006.
14. Clarke DW, Mohtadi C, Tuffs PS. Generalized Predictive Control-Part II Extensions and interpretations. Automatica. 1987;23(2):149–60.
15. Stefanopoulou a G, Kolmanovsky I, Freudenberg JS. Control of variable geometry turbocharged diesel engines for reduced emissions. Proc 1998 Am Control Conf ACC IEEE Cat No98CH36207 [Internet]. 2000;3(4):733–45. Available from: http://ieeexplore.ieee.org/xpls/abs_all.jsp?arnumber=852917
16. Jankovic M, Jankovic M, Kolmanovsky I. Constructive Lyapunov control design for turbocharged diesel engines. IEEE Trans Control Syst Technol. 2000;8(2):288–99.
17. Abidi I, Bosche J, El Hajjaji A, Aitouche A. Control of a turbocharged diesel engine with EGR system using Takagi-Sugeno's approach. In: 2012 20th Mediterranean Conference on Control and Automation, MED 2012 - Conference Proceedings. 2012. p. 960–5.
18. Oh B, Lee M, Park Y, Sohn J, Won J, Sunwoo M. VGT and EGR Control of Common-Rail Diesel Engines Using an Artificial Neural Network. J Eng Gas Turbines Power. 2012;135(1).

19. Kuzmych O, Aitouche A, Cheng L. Robust nonlinear control design for turbocharged biodiesel engine. In: 2013 3rd International Conference on Systems and Control, ICSC 2013. 2013. p. 395–400.
20. Bai L, Yang M. Coordinated Control of EGR and VNT in Turbocharged Diesel Engine Based on Intake Air Mass Observer. Neural Networks. 2009;(724).
21. Simani S, Bonfè M. Fuzzy modelling and control of the air system of a diesel engine. Adv Fuzzy Syst. 2009;
22. Mastrovito, M, Gaballo, L,Dambrossion, L. Diesel engine variable-geometry turbine turbocharger controlled by a multi-agent based algorithm. Proc Inst Mech Eng D J Auto. 2008;222:1459-1470.
23. You, K, Wei L, Jiang, K. A fuzzy logic urea dosage controller design for two-cell selective catalytic reduction systems. ISA Transactions. 2018;78:21-30.
24. Gnanasekaran, S. Prediction of CI engine performance, emission and combustion characteristics using fish oil as biodiesel at different injection timing using fuzzy logic. Fuel. 2016;183:214-229.
25. Zamboni G, Capobianco M. Experimental study on the effects of HP and LP EGR in an automotive turbocharged diesel engine. Appl Energy. 2012;94:117–28.
26. Lundqvist U, Smedler G, Stålhammar P. A Comparison Between Different EGR Systems for HD Diesel Engines and Their Effect on Performance , Fuel Consumption and. Engineering. 2011;2000(724).
27. Langridge S, Fessler H. Strategies for High EGR Rates in a Diesel Engine. SAE Int. 2002;(724).
28. Dimitriou P, Turner J, Burke R, Copeland C. The benefits of a mid-route exhaust gas recirculation system for two-stage boosted engines. Int J Engine Res. 2017;
29. Shayler PJ, Leong DKW, Murphy M. Contributions to engine friction during cold, low speed running and the dependence on oil viscosity. SAE Trans [Internet]. 2005;114(3):1191–201. Available from: http://cat.inist.fr/?aModele=afficheN&cpsidt=17553819
30. Zapf H. A contribution towards heat transfer analysis during medium exchange phase of a 4-stroke diesel engine (Beitrag zur Untersuchung des Wärmeübergangs während des Ladungswechsels im Viertakt-Dieselmotor). MTZ. 1969;30:461–5.
31. Sugeno M. An introductory survey of fuzzy control. Inf Sci (Ny). 1985;36(1–2):59–83.
32. Sugeno M. Industrial applications of fuzzy control. Elsevier Sci Pub Co. 1985;
33. Ishizuka S, Kajiwara I, Sato J, Hanamura Y, Hanawa S. Model-free adaptive control scheme for EGR/VNT control of a diesel engine using the simultaneous perturbation stochastic approximation. Trans Inst Meas Control. 2017;39(1).
34. Divekar PS, Chen X, Tjong J, Zheng M. Energy efficiency impact of EGR on organizing clean combustion in diesel engines. Energy Convers Manag. 2016;112:369–81.
35. Zadeh L a. Fuzzy sets. Inf Control. 1965;8(3):338–53.
36. Hong S, Park I, Chung J, Sunwoo M. Gain scheduled controller of EGR and VGT systems with a model-based gain scheduling strategy for diesel engines. In: IFAC-PapersOnLine. 2015. p. 109–16.
37. Cheng L, Wang W, Aitouche A, Peng Z. Robustness evaluation of real-time fuzzy logic control of the VGT and EGR on a diesel engine. In: 2015 23rd Mediterranean Conference on Control and Automation, MED 2015 - Conference Proceedings. 2015. p. 211–7.
38. Hosoz M, Ertunc HM, Karabektas M, Ergen G. ANFIS modelling of the performance

and emissions of a diesel engine using diesel fuel and biodiesel blends. Appl Therm Eng. 2013;60(1–2):24–32.
39. Nikzadfar K, Shamekhi AH. An extended mean value model (EMVM) for control-oriented modeling of diesel engines transient performance and emissions. Fuel. 2015;154:275–92.
40. Quérel C, Grondin O, Letellier C. Semi-physical mean-value NOx model for diesel engine control. Control Eng Pract. 2015;40:27–44.

Appendix

The soot formation provided by the AVL 439 opacimeter are given in % opacity. On the other hand, AVL-BOOST simulation software provides reading in g/kWh.

The normalization of soot emission for comparison purposes was performed using the following equation.

$$Normalized\ Soot\ (\%) = Soot_{sim}(\frac{g}{kWh})\ /\ \text{Conversion Factor}$$

The Conversion Factor was estimated using the following approach.

Considering at a particular high-fidelity engine operating point with very accurate predictions of NOx, fuel consumption and power output and assuming that,

$$Normalized\ Soot\ (\%) = Soot_{exp}(\%)$$

then,

$$\text{Conversion Factor} = \frac{Soot_{sim}(\frac{g}{kWh})}{Normalized\ Soot\ (\%)} = \frac{Soot_{sim}(\frac{g}{kWh})}{Soot_{exp}\ (\%)}$$

Validating that the Conversion Factor is of the same magnitude at a second operating point increases the fidelity of the normalization approach.

Although this approach is not of the highest accuracy, it is believed that is the optimum approach for comparing the soot formation readings given by the simulation software against the readings provided by the AVL opacimeter.